



Fixel-Based Analysis Reveals Whole-Brain White Matter Abnormalities in Cervical Dystonia

Giuseppe Zito, Clément Tarrano, Salim Ouarab, Prasanthi Jegatheesan, Asya Ekmen, Benoît Béranger, Romain Valabregue, Cécile Hubsch, Sophie Sangla, Cécilia Bonnet, et al.

► To cite this version:

Giuseppe Zito, Clément Tarrano, Salim Ouarab, Prasanthi Jegatheesan, Asya Ekmen, et al.. Fixel-Based Analysis Reveals Whole-Brain White Matter Abnormalities in Cervical Dystonia. *Movement Disorders*, 2023, 38 (7), pp.1187-1196. 10.1002/mds.29425 . hal-04237577

HAL Id: hal-04237577

<https://hal.science/hal-04237577>

Submitted on 11 Oct 2023

HAL is a multi-disciplinary open access archive for the deposit and dissemination of scientific research documents, whether they are published or not. The documents may come from teaching and research institutions in France or abroad, or from public or private research centers.

L'archive ouverte pluridisciplinaire **HAL**, est destinée au dépôt et à la diffusion de documents scientifiques de niveau recherche, publiés ou non, émanant des établissements d'enseignement et de recherche français ou étrangers, des laboratoires publics ou privés.

RESEARCH ARTICLE

Fixel-Based Analysis Reveals Whole-Brain White Matter Abnormalities in Cervical Dystonia

Giuseppe A. Zito, PhD,¹ Clément Tarrano, MD,^{2,3} Salim Ouarab, MSc,² Prasanthi Jegatheesan, PhD,² Asya Ekmen, MD,² Benoît Béranger, MSc,⁴ Romain Valabregue, MSc,⁴ Cécile Hubsch, MD, PhD,² Sophie Sangla, MD,² Cécilia Bonnet, MD, PhD,² Cécile Delorme, MD,² Aurélie Méneret, MD, PhD,^{2,5} Bertrand Degos, MD, PhD,^{2,6,7} Floriane Bouquet, MD,² Marion Apoil Brissard, MD,⁸ Marie Vidailhet, MD,^{2,5} Dominique Hasboun, MD,^{2,3} Yulia Worbe, MD, PhD,^{2,9} Emmanuel Roze, MD, PhD,^{2,5} and Cécile Gallea, PhD^{2*}

¹Swiss Paraplegic Research, Nottwil, Switzerland

²Movement Investigation and Therapeutics Team, Paris Brain Institute, Sorbonne University, Inserm U1127, CNRS UMR7225, Paris, France

³Department of Neurology, Assistance Publique-Hôpitaux de Paris, Pitié-Salpêtrière Hospital, Paris, France

⁴Center for Neuroimaging Research (CENIR), Paris Brain Institute, Sorbonne University, Inserm U1127, CNRS UMR 7225, Paris, France

⁵DMU Neurosciences, Assistance Publique-Hôpitaux de Paris, Paris, France

⁶Neurology Unit, AP-HP, Avicenne University Hospital, Sorbonne Paris Nord, Bobigny, France

⁷Center for Interdisciplinary Research in Biology, Collège de France, CNRS UMR7241/INSERM U1050, Université PSL, Paris, France

⁸Université de Caen Normandie, Caen, France

⁹Department of Neurophysiology, Saint-Antoine Hospital, Assistance Publique-Hôpitaux de Paris, Paris, France

ABSTRACT: Background: Cervical dystonia (CD) is a form of isolated focal dystonia typically associated to abnormal head, neck, and shoulder movements and postures. The complexity of the clinical presentation limits the investigation of its pathophysiological mechanisms, and the neural networks associated to specific motor manifestations are still the object of debate.

Objectives: We investigated the morphometric properties of white matter fibers in CD and explored the networks associated with motor symptoms, while regressing out nonmotor scores.

Methods: Nineteen patients affected by CD and 21 healthy controls underwent diffusion-weighted magnetic resonance imaging. We performed fixel-based analysis, a novel method evaluating fiber orientation within specific fiber bundles, and compared fiber morphometric properties between groups. Moreover, we correlated fiber morphometry with the severity of motor symptoms in patients.

Results: Compared to controls, patients exhibited decreased white matter fibers in the right striatum. Motor symptom severity negatively correlated with white matter fibers passing through inferior parietal areas and the head representation area of the motor cortex.

Conclusions: Abnormal white matter integrity at the basal ganglia level may affect several functional networks involved, for instance, in motor preparation and execution, visuomotor coordination, and multimodal integration. This may result in progressive maladaptive plasticity, culminating in overt symptoms of dystonia. © 2023 The Authors. *Movement Disorders* published by Wiley Periodicals LLC on behalf of International Parkinson and Movement Disorder Society.

Key Words: cervical dystonia; diffusion-weighted imaging; fixel-based analysis

This is an open access article under the terms of the [Creative Commons Attribution-NonCommercial-NoDerivs](#) License, which permits use and distribution in any medium, provided the original work is properly cited, the use is non-commercial and no modifications or adaptations are made.

*Correspondence to: Dr. Cécile Gallea, Paris Brain Institute (ICM)-Salpêtrière Hospital, 47-83 Boulevard de l'Hôpital, 75013 Paris, France; E-mail: cecile.gallea.icm@gmail.com; cecile.gallea@icm-institute.org

Yulia Worbe, Emmanuel Roze, and Cécile Gallea have contributed equally to this work.

Relevant conflicts of interest/financial disclosures: The authors declare no conflict of interest.

Funding agencies: This work was funded by the Swiss National Science Foundation (P400PM_183958 and P5R5PM_203160/1), AMADYS, Fondation Brou de Laurière, and Merz-Pharma. This project was also supported by "Agence Nationale de la Recherche (ANR)" under the frame of the European Joint Programme on Rare Diseases (EJP RD, ANR-16-CE37-0003-03).

Received: 6 February 2023; **Revised:** 4 April 2023; **Accepted:** 12 April 2023

Published online 6 May 2023 in Wiley Online Library (wileyonlinelibrary.com). DOI: 10.1002/mds.29425

Cervical dystonia (CD) is a form of focal dystonia characterized by patterned, directional, and often sustained contractions of the neck muscles, which produce abnormal head posture or repetitive head movements.¹ Its pathogenesis involves maladaptive plasticity and abnormal sensorimotor processing.^{2,3} The complexity of its clinical presentation, as well as the large variety of potential causative factors, limits the investigation of its mechanism. Besides the classical “motor” phenotype, nonmotor manifestations of CD, such as anxiety, depression, sleep disorders, cognitive impairment, and pain, have been observed in patients.^{4,7} A clear dissociation between motor and nonmotor manifestations of CD has not been established yet.^{4,6}

CD has been historically seen as a disorder resulting from abnormal functioning of the cortico-basal ganglia-cerebellar networks,⁸ but this view has been recently challenged by several neuroimaging studies that have shown widespread abnormalities in several other brain regions.^{3,9-11} For instance, in CD patients compared to healthy controls (HC), a reduction in activation of parietal, premotor, and cingulate cortices has been found during movement imagery,¹¹ as well as increased activity in cerebellar and temporal regions and decreased activity in somatosensory and parietal regions, in response to a motor task.³ CD is now considered a large-scale network disorder, affecting the connectivity of multiple cortical and subcortical brain areas, beyond the motor system.^{9,12} However, the questions on which specific brain networks are impaired in CD and how they affect motor behavior, independent of nonmotor manifestations, are still open.

Interestingly, whereas the results of functional magnetic resonance imaging analyses have been consistent across the literature, studies on structural connectivity have reported conflicting findings.¹³ For instance, some voxel-based analysis (VBA) studies have found an increase in fractional anisotropy (FA) and mean diffusivity (MD) in the prefrontal cortex, thalamus, and striatum in CD patients,^{14,15} whereas others have reported a decrease in FA and MD in the corpus callosum, globus pallidus, and striatum¹⁴⁻¹⁶ (for a full review, see Ramdhani and Simonyan¹³). VBA approaches present some limitations. For instance, they are based on T1-weighted images and thus are not able to (1) distinguish among multiple populations of fibers within the same voxel and (2) account for fiber orientation spanning across several voxels.¹⁷ This information is crucial, as up to 90% of white matter voxels contain two or more fiber populations,¹⁸ each with its specific orientation. To overcome this limitation, a new method based on diffusion-weighted imaging (DWI), called fixel-based analysis (FBA), has been recently proposed to study morphometric properties of fiber pathways.^{17,19} The concept of fixel, referring to a specific population of fibers within a single voxel, is used as a parallel of voxel

in standard VBA, and a novel statistical framework called connectivity-based fixel enhancement (CFE) is employed to perform statistical comparisons of the white matter tracts.¹⁷ Important insights into the pathophysiology of other neurological conditions, such as Alzheimer’s disease²⁰ or multiple sclerosis,²¹ have been gained using this method, but no study on fiber pathways has been conducted in CD.

In this exploratory study, we examined abnormalities in white matter fibers in CD patients and investigated their potential link with the severity of dystonia, while accounting for nonmotor manifestations as nuisance covariates. We combined FBA and VBA approaches to compare white matter properties between CD patients and HC. Our working hypothesis was that CD patients show differences in white matter tracts that encompass widespread networks across the entire brain. Due to the exploratory nature of this study, no hypothesis was postulated on the directionality of these differences. We then performed a correlation analysis to study the relation between white matter fiber abnormalities and clinical manifestations of CD and explored the brain networks associated to the severity of dystonia.

Patients and Methods

Subjects and General Procedure

We recruited 19 CD patients (7 men, mean age = 49.3 ± 5.6 years) and 21 sex- and age-matched HCs (9 men, mean age = 45.3 ± 10.6 years) through the Pitié-Salpêtrière Hospital, Paris, France. Inclusion criteria for patients were a diagnosis of isolated focal CD according to Axis I and idiopathic CD according to Axis II,²² no botulinum toxin injection within 3 months before the examination, and stable pharmacological treatment for at least 1 month before the experiment. We excluded patients with severe tremor or essential tremor to ensure good imaging quality. Symptom severity in CD was assessed during the inclusion using the Toronto Western Spasmodic Torticollis Rating Scale (TWSTRS), subscale for severity.²³ All participants were also screened for mood disturbances using the Beck Depression Inventory (BDI),²⁴ and general intelligence quotient (IQ) was assessed using the Wechsler Adult Intelligence Scale—Full Scale (WAIS-IV FSIQ).²⁵ Between-group differences in age, WAIS, and BDI score were assessed using independent-sample *t* tests, and differences in the ratio between male and female participants were assessed using χ^2 tests.

The study was carried out in accordance with the latest version of the Declaration of Helsinki and approved by the local ethics committee (approval number: C17-04-AU 1360, [ClinicalTrials.gov](https://clinicaltrials.gov) ID: NCT03351218). All participants provided written informed consent before inclusion.

Neuroimaging Acquisition Parameters and Preprocessing

Participants were asked to lie still in a 3-T MAGNETOM Prisma scanner (Siemens, Erlangen, Germany) while fixating on a cross displayed on a screen during the MR session. Eye-tracking was employed to monitor their gaze. We acquired DWI data and one structural image in one single session and a 64-channel head coil. The structural image was acquired using a T1-weighted MP2RAGE sequence with repetition time (TR) = 5 seconds, echo time (TE) = 2.96 ms, inversion time = 700/2500 ms, field of view = 232×256 in plane $\times 176$ slices, 1 mm isotropic, and Ipat acceleration factor = 3. DWI data (echo planar imaging [EPI] 2D) were acquired using the following parameters: spatial resolution = $1.75 \times 1.75 \times 1.75$ mm, dimensions = $118 \times 118 \times 81$ mm, EPI factor = 128, TR = 3.5 s, TE = 75 ms, flip angle = 90° , a multiband factor of 3, and 6/8 partial Fourier transform. We acquired three different shells, 60 directions at $b = 2000$, 32 directions at $b = 1000$, and 8 directions at $b = 300$. The gradient directions were interleaved with four non-diffusion-weighted reference images (b -value = 0 s/mm²), including a b_0 image with opposite phase-encode blip to correct image distortions based on individual susceptibilities.

Image preprocessing was performed as follows: T1-weighted images were background denoised,^{26,27} segmented, and normalized to the Montreal Neurological Institute space using the Computational Anatomy Toolbox (CAT12—<http://www.neuro.uni-jena.de/cat/>) extension for SPM12 (<https://www.fil.ion.ucl.ac.uk/spm/software/spm12/>). We extracted total intracranial volume (TIV) to be used in later analyses. DWI data were first denoised, that is, eddy current correction from FMRIB Software Library (FSL, Analysis Group, FMRIB, Oxford, UK),²⁸ and Gibbs artifact was removed using Mrtrix3.²⁹ The $b = 0$ volumes were then extracted and combined with the opposition phase direction volumes, and EPI distortion correction was performed using “topup tool” from FSL.³⁰ We then corrected for motion and eddy current using “eddy tool” from FSL. We then used the “noddi matlab toolbox” to fit the NODDI model to the multi-shell preprocessed diffusion data, as previously described.³¹

Analysis of Fixel-Based and Voxel-Based Morphometry

We performed FBA¹⁹ and investigated white matter fiber-specific differences between CD patients and HCs. After image preprocessing, we computed for each single subject a fiber orientation distribution (FOD) and used this information to derive a study-specific, unbiased template representing the population FOD. All single-subject FODs were registered with the population template, which was used as the reference image for the main analyses. We then computed a white matter

template mask and segmented the fixels from the FOD template. We used CFE to generate a whole-brain tractogram from the FOD template and spherical deconvolution-informed filtering of tractograms to reduce tractography bias.³² Finally, we calculated fiber density (FD), a measure of the within-voxel intra-axonal volume of a fiber bundle, and fiber bundle cross-section (FC), a measure of the macroscopic, between-voxel intra-axonal volume of the fiber bundle. A third measure combining FD and FC, that is, FDC, was not included in the analysis, as it did not provide additional information over the single FD and FC. We performed connectivity-based smoothing and statistical inference with CFE, using 2 million streamlines and default parameters (smoothing = 10-mm full width at half maximum [FWHM], $C = 0.5$, $E = 2$, and $H = 3$).¹⁷

To perform group comparisons, we defined regions of interest (ROIs) based on the Brainnetome³³ and the Spatially Unbiased Infratentorial toolbox³⁴ atlases and sorted them into different families, based on functional specialization of brain areas, namely sensorimotor region, limbic region, frontal region, basal ganglia/thalamic region, visual region, temporoparietal region, cerebellum, and brainstem (Table S1). For each ROI family, we then studied statistical differences between CD patients and HCs in FD and FC, respectively, using a general linear model (GLM). To account for small intersubject differences between groups, we included BDI score, TIV, age, and sex as nuisance regressors. We did not include medication status among the regressors due to the high heterogeneity in the drugs prescribed to the patients, in comparison to our sample size. We applied family-wise error (FWE) correction for multiple comparisons using nonparametric permutation testing with 5000 permutations.³⁵ Significance threshold was set at $P_{\text{corrected}} < 0.050$.

We also performed a standard VBA to study changes in white matter volume between CD patients and HCs. After preprocessing, the normalized white matter volumes obtained during the segmentation were smoothed using an 8-mm FWHM kernel. We implemented a GLM testing between-group differences in the ROIs presented in Table S1. BDI score, TIV, age, and sex were included as nuisance regressors. An uncorrected threshold of $P < 0.001$ was selected at peak level, and an FWE threshold of $P_{\text{corrected}} < 0.05$ was applied at cluster level. This analysis was performed using SPM12.

Correlation Analysis

To study the relation between motor manifestations of CD and structural FBA metrics, we performed a correlation analysis. We implemented a GLM in the ROI families provided in Table S1 and tested clusters of FD and FC showing a significant correlation with the

TABLE 1 Clinical and demographic information

Demographic and clinical parameters	HC (N = 21)	CD (N = 19)	Statistics
Sex (male/female)	9/12	7/12	$\chi(1) = 0.15, P = 0.698$
Age (y, mean \pm SD)	45.3 \pm 10.6	47.3 \pm 8.6	$t(38) = 0.66, P = 0.512$
WAIS-IV	116.3 \pm 4.8	116.3 \pm 5.6	$t(38) = 0.02, P = 0.984$
BDI	0.9 \pm 1.3	3.7 \pm 4.3	$t(38) = 2.84, P = 0.007$
TWSTRS	—	18.0 \pm 4.3	—
Overall medication, N (% of CD)	—	19 (100%)	—
BoT, N (% of TD) ^a	—	17 (89.5%)	—
Others (tramadol, levothyroxine, diazepam, escitalopram, alprazolam, tetrazepam, fluoxetine, citalopram, clomipramine, lamotrigine—[N, % of CD])	—	4 (21.0%)	—

Note: Comparison of clinical and demographic scores between groups.

Abbreviations: HCs, healthy controls; CD, cervical dystonia; SD, standard deviation; WAIS, Wechsler Adult Intelligence Scale; BDI, Beck Depression Inventory; TWSTRS, Toronto Western Spasmodic Torticollis Rating Scale; BoT, botulinum toxin injection.

^aLast BoT administered at least 3 months before the experiment.

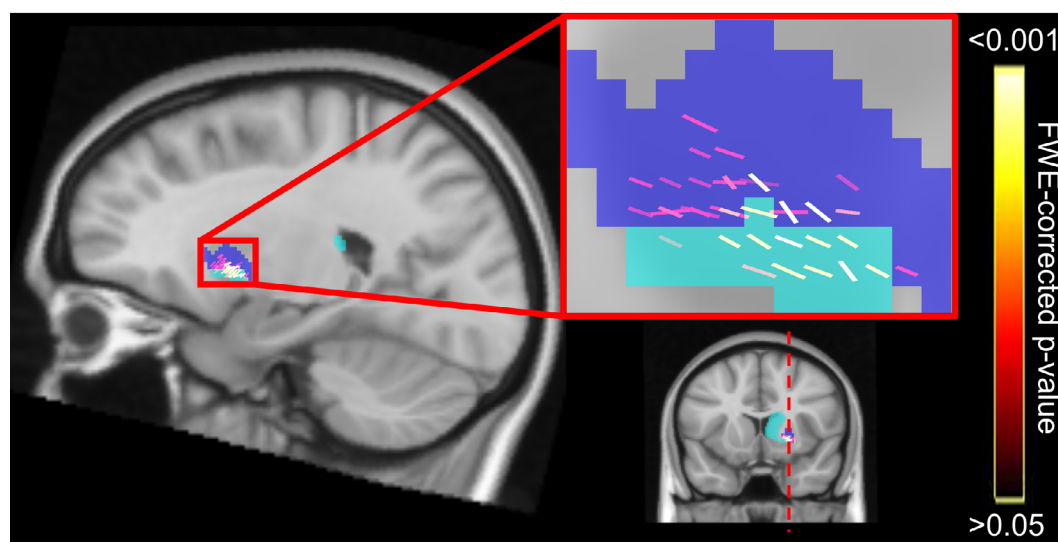


FIG. 1. Results of the comparison between CD patients and HCs. Decreased FD in CD patients in the right striatum. Clusters represent the P -values corrected for multiple comparisons with FWE permutation testing. Zoomed-in image shows fixel orientation. Light-blue shade identifies the nucleus caudate, and dark-blue shade identifies the putamen. CD, cervical dystonia; FD, fiber density; FWE, family-wise error; HCs, healthy controls. [Color figure can be viewed at wileyonlinelibrary.com]

TWSTRS in CD patients. BDI scores, TIV, age, and sex were included as nuisance regressors. FWE threshold of $P_{\text{corrected}} < 0.050$, corrected using nonparametric permutation testing with 5000 permutations,³⁵ was applied. All FBAs were performed using MRtrix3.²⁹

Identification of the Affected White Matter Tracts

To better appreciate all the fiber pathways that were mainly affected, we reconstructed a whole-brain connectome and highlighted the tracts passing

through the regions of local structural alterations identified in the main FBA. In particular, we selected the regions showing differences between CD patients and HCs, as well as the regions correlating with TWSTRS, as seed ROIs and the areas provided in Table S1 as target ROIs (considered as bilateral ROIs except for the brainstem). For each voxel of the seed ROIs, we considered 5000 fiber streamlines with the following tracking parameters: step size = 0.5 mm, maximum trace length = 500 mm, and curvature threshold = $\pm 80^\circ$. This yielded $5000 \times n$ streamlines from the seed ROIs, where n is the number of voxels

in each ROI.³⁶ We then calculated the connectivity probability between the seed ROI i and target ROI j as the ratio between the number of fibers passing

through j and the total number of fibers from i .³⁷ Similarly, we calculated the inverse probability, that is, the probability from j to i , which is not equal to that from i to j . We then computed the connectivity probability between region i and region j as the average of the two probabilities.^{38,39} For each subject, we estimated a $k \times 15$ connectivity matrix, where k is the number of seed ROIs and 15 is the target ROIs. For each seed ROI, we finally considered the top 20% regions holding the highest probability of connection⁴⁰ and identified the corresponding tracts. When a cluster belonged to one of the target ROIs, for example, a cluster in the PrG and a target ROI in the sensorimotor region, we additionally performed an atlas-based tractography with specific seeds to confirm that the tract crossed the cluster without bias; that is, we excluded the specific fixels within the cluster from the target ROI.

Results

No significant differences were found in age, IQ, and sex ratio between male and female participants (Table 1), therefore confirming the similarity between the two groups with regard to overall intellectual functioning. Mean BDI score in CD patients was 3.7 ± 4.3 , which cannot be considered as indicative of clinical depression,²⁴ yet it was significantly higher compared to HCs. Severity of motor symptoms in patients was 18.0 ± 4.3 , as assessed using the TWSTRS. A detailed description of the clinical population is presented in Table S2.

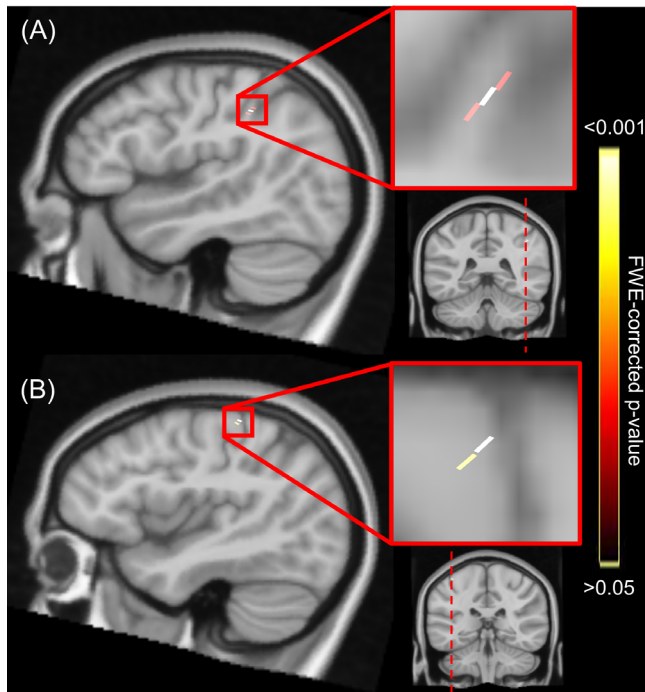


FIG. 2. Results of correlation analysis in CD patients. (A) Negative correlation between TWSTRS and FD in the right inferior parietal lobule. (B) Negative correlation between TWSTRS score and FD in the left precentral gyrus. Clusters represent the P -values corrected for multiple comparisons with FWE permutation testing. Zoomed-in image shows fixel orientation. CD, cervical dystonia; FD, fiber density; FWE, family-wise error; TWSTRS, Toronto Western Spasmodic Torticollis Rating Scale. [Color figure can be viewed at wileyonlinelibrary.com]

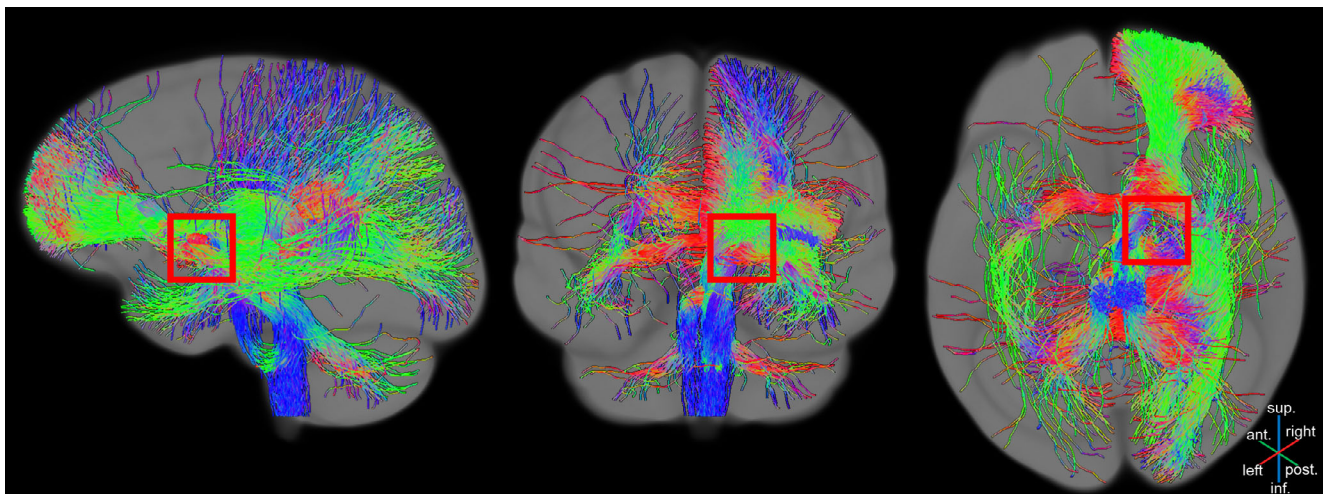


FIG. 3. Affected connectivity pathways from the comparison between CD patients and HCs. The fibers passing through the significant fixels are shown. Red squares are centered over the areas of significant fixels. The color of the fibers is representative of their direction (blue for inferior-superior tracts, green for anterior-posterior tracts, and red for left-right tracts). CD, cervical dystonia; HCs, healthy controls. [Color figure can be viewed at wileyonlinelibrary.com]

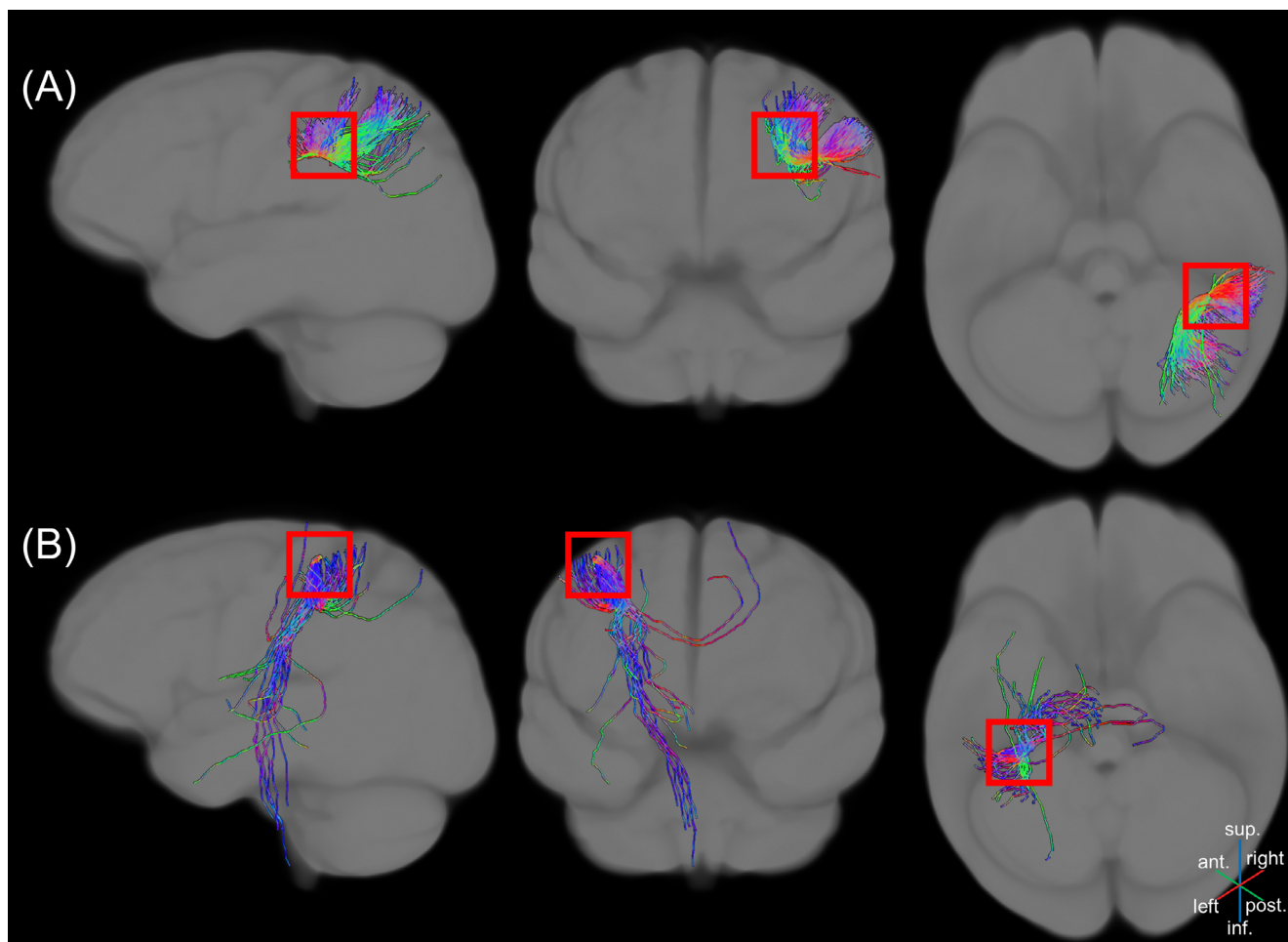


FIG. 4. Affected connectivity pathways from the correlation analysis. The fibers passing through the significant fixels are shown. Red squares are centered over the areas of significant fixels. The color of the fibers is representative of their direction (blue for inferior–superior tracts, green for anterior–posterior tracts, and red for left–right tracts). **(A)** Short-association fibers within the posterior parietal cortex. **(B)** Corticospinal tract. [Color figure can be viewed at [wileyonlinelibrary.com](https://onlinelibrary.wiley.com/doi/10.1002/mds.29425)]

Fixel-Based, Voxel-Based, and Correlation Analyses

The results of FBA evidenced decreased FD in CD patients, compared to HCs, in the right striatum, with peak in the right putamen ($P_{\text{peak}} = 0.014$; Fig. 1).

Standard VBA revealed no significant differences in white matter volume between CD patients and HCs.

Moreover, CD patients showed a significant negative correlation between TWSTRS and FD in the right rostro-dorsal segment 40 of the inferior parietal lobule (IPL, $P_{\text{peak}} = 0.005$; Fig. 2A), as well as in the left PrG, head and face representation area ($P_{\text{peak}} = 0.036$; Fig. 2B).

Identification of White Matter Tracts

The affected pathways were derived from the top 20% regions with the highest connectivity probability and are shown in Figures 3 and 4 for the group comparison and the correlation analysis, respectively. The

full probability of connections is shown in Figure S1. The tracts that showed differences between CD patients and HCs were widespread over the whole brain and mostly affected the striato-cortical connectivity and the temporoparietal, frontal, and cerebellar connections, as well as the sensory tract (Fig. 3). TWSTRS negatively correlated with short-association fibers within the posterior parietal cortex (PPC; Fig. 4A) and the corticospinal tract (Fig. 4B).

Discussion

Our results highlighted morphometric abnormalities in white matter fibers of patients with CD in widespread brain regions.^{9,12} In line with existing literature on other forms of dystonia, we propose a pathophysiological model of CD where discrete functional and structural abnormalities likely underlie the divergent mechanisms in the development of distinct clinical symptomatology.⁴¹ CD patients exhibited decreased FD

in the basal ganglia, more specifically in the right striatum, which affected the connectivity of widespread regions, including the right frontal and temporoparietal connections. Interestingly, when accounting for non-motor manifestations, areas in the PPC and the motor areas correlated with motor severity in patients.

Our analytical method allowed us to investigate the orientation of specific white matter anatomical features. In particular, FD addresses changes in white matter volume within a given voxel, whereas FC addresses changes that concern the number of voxels that the entire fiber bundle occupies. FD may reflect axonal volume, whereas FC may depict a scenario where, after axonal loss, the extra-axonal space may be filled with extracellular matrix.¹⁹ However, such inferences at axonal level are speculative, as this method does not provide information on single neurons, but on fiber pathways, and its results should be rather interpreted as the ability of a fiber pathway to relay information. In standard VBA, measures of FA and MD are typically used to address axonal integrity, myelination, axon diameter, and density.⁴² Yet, when investigating white matter, a difference in these parameters does not necessarily reflect a difference in the fiber properties. For instance, if two groups differ locally in volume along the length of a fiber, this does not imply a difference in the number of axons. In contrast, if the volume difference is perpendicular to the fiber orientation (ie, a difference in FC), this does imply a difference in the number of axons. It is therefore essential to account for fiber orientation when investigating the morphology of white matter.¹⁹ FBA shifts the focus from the morphometry of white matter areas to the morphometry of white matter tracts and accounts for fiber orientation within a specific fiber bundle. By following these directional estimates, FBA makes it possible to accurately trace the pathways of underlying fiber bundles, therefore to study the actual connectivity of distinct brain areas.⁴³ However, one limitation of both VBA and FBA is that they do not allow us to disentangle causal, compensatory, and epiphenomenal relationships across the different networks,² and we cannot infer whether the reduced FD and FC are a consequence of the disorder or rather reflecting the pathogenesis of CD. Of note, our b-value (2000 s/mm²) is smaller than the recommendation for optimal characterization of FD.⁴⁴ However, clinical studies on FBA have also acquired DWI data at b = 2000 s/mm²,^{45,46} and we believe that the quality of our data is sufficient to infer morphometric properties of white matter fibers. ■

Abnormal White Matter Fibers in Cervical Dystonia

We previously demonstrated abnormal functional connectivity of the PrG in CD patients, specific to the affected body representation area.⁴⁷ Here we expand the knowledge of aberrant activity in specific functional

networks in CD by showing that such aberrations are related to changes in white matter fibers across the whole brain. There is converging evidence of a role of the right striatum and primary motor cortex in dystonia, as shown in a recent meta-analysis on structural and functional abnormalities in CD.⁴⁸ The decreased connectivity of the striatum evidenced in our study supports a framework where aberrant white matter integrity in the basal ganglia might induce a distortion of the motor information reaching the cortex.⁴⁹ This may eventually lead to dysfunction in somatosensory processing in focal dystonia^{50,51} and ultimately to unwanted and excessive motor output. Interestingly, our results showed alterations mostly affecting the right hemisphere. The consistency of right-sided findings may suggest that CD is associated to an underlying asymmetric pathogenesis, possibly due to compensatory responses across hemispheres.^{52,53} These results could be due to a bias in the laterality of the head position, as our sample comprised 12 patients with right- and 7 patients with left-sided head twist (Table S2). However, we suggest that this is unlikely. The head twist is often associated with co-contraction of muscles from both sides of the body. Interpreting our results in terms of the laterality of cortical representation of neck muscles associated with the symptoms is thus challenging. The relationship between the laterality of the symptoms and the laterality of the neuroimaging findings is difficult to investigate, pending a consensual and robust definition of symptom laterality that could be applied in any form of CD. Instead, the laterality of white matter tract abnormalities in CD could be considered in terms of hemispheric dominance. Neuroimaging findings have shown that right-hemispheric damage is associated with deficits in motor and bodily awareness.⁵⁴⁻⁵⁶ Particularly, regardless of the laterality of the limb involved in the task, the inferior parietal cortex is activated during proprioceptive (kinesthetic) processing of muscle spindle afferent inputs, which generate somatic sensation in a right-side dominant manner.^{57,58} The right IPL is likely an important node in the brain network associated with proprioceptive/motor awareness of limb movement,⁵⁹ a function that could be altered in CD due to the persistence of their symptoms. One potential limitation of the current analysis is that some patients were treated with centrally acting drugs, which might have influenced the results.

Correlation with Motor Manifestations of Cervical Dystonia

Some abnormalities in the white matter fibers correlated with motor symptoms in the corticospinal tract and PPC, regardless of the degree of nonmotor manifestations (BDI scores). This finding is novel and further strengthens the hypothesis of CD as network disorder,

where motor manifestations reflect abnormal connectivity of distinct brain regions beyond the sensorimotor system. However, when accounting for potential confounds in our analysis, we included only measures of mood, and we did not assess the specific effects of comorbid sleep, fatigue, apathy, and anxiety, which can be considered as part of the clinical presentation of CD. This could have potentially limited the interpretation of our results.

The correlation between TWSTRS and parietal regions might be related to cortico-cortical projections arising from the IPL and terminating in the PPC through short-association fibers. These fibers have been previously isolated in healthy subjects.⁶⁰ An alteration in these fibers (lower FD) linked to symptom severity (higher TWSTRS) suggests that the PPC of patients with CD may undergo intrinsic loss of functionality related to visuomotor processing. This may in turn influence the output of the motor cortex, contributing to dystonic manifestations.⁶¹ This hypothesis is supported by previous studies showing decreased parietal activation during reaching movements in CD^{11,61} and alterations in motor and parietal regions in task-specific focal dystonia.⁶² It is then possible that parietal dysfunctions may affect visuomotor integration, leading to the inability to initiate movement promptly.^{63,64} Furthermore, these white matter pathways are involved in the integration of visual and proprioceptive feedback,⁶⁵ further strengthening the hypothesis of impaired visuomotor abilities in CD. The IPL is considered to contain action representation or sensorimotor schemes.⁶⁶ Functionally, it is possible that abnormal sensory processing in the superior parietal cortex is associated with abnormal action representation in the inferior parietal cortex, as already observed in other forms of focal dystonia.^{67,68} Alternatively, these alterations may be related to secondary disturbances of visual processing, related to abnormal head position induced by dystonia.

Overall, our study showed widespread abnormalities in several brain networks related to specific aspects of CD, challenging the classical view of a purely cortico-basal ganglia-cerebellar dysfunction.⁶⁹ An impairment of higher-order motor control from the basal ganglia may propagate to several functional networks involved, for instance, in motor preparation and execution, multimodal integration, and visuomotor coordination. Malfunctioning of sensorimotor feedback, alongside an abnormal excitability of motor circuits at different levels, may thus result in a progressive maladaptive plasticity in cortical and subcortical structures, culminating in overt symptoms of dystonia.^{2,9,70}

Acknowledgments: We thank the Swiss National Science Foundation (SNSF), the Paris Brain Institute, and the University Hospitals Pitié-Salpêtrière for support. We also thank all the participants of our study.

Data Availability Statement

The data that support the findings of this study are available from the corresponding author upon reasonable request.

References

- Geyer HL, Bressman SB. The diagnosis of dystonia. *Lancet Neurol* 2006;5(9):780–790.
- Quartarone A, Hallett M. Emerging concepts in the physiological basis of dystonia. *Mov Disord* 2013;28(7):958–967.
- Burciu RG, Hess CW, Coombes SA, et al. Functional activity of the sensorimotor cortex and cerebellum relates to cervical dystonia symptoms. *Hum Brain Mapp* 2017;38(9):4563–4573.
- Matteo C, Daniele B, Isabella B, et al. Motor and non-motor subtypes of cervical dystonia. *Parkinsonism Relat Disord* 2021;88:108–113.
- Klingelhofer L, Martino D, Martinez-Martin P, et al. Nonmotor symptoms and focal cervical dystonia: observations from 102 patients. *Basal Ganglia* 2014;4(3–4):117–120.
- Yang J, Shao N, Song W, et al. Nonmotor symptoms in primary adult-onset cervical dystonia and blepharospasm. *Brain Behav* 2017;7(2):e00592.
- Stamelou M, Edwards MJ, Hallett M, Bhatia KP. The non-motor syndrome of primary dystonia: clinical and pathophysiological implications. *Brain* 2012;135(6):1668–1681.
- Berardelli A, Rothwell J, Hallett M, Thompson P, Manfredi M, Marsden C. The pathophysiology of primary dystonia. *Brain* 1998;121(7):1195–1212.
- Battistella G, Termsarasab P, Ramdhani RA, Fuertinger S, Simonyan K. Isolated focal dystonia as a disorder of large-scale functional networks. *Cereb Cortex* 2015;27((2)):bhv313.
- Delnooz CC, Pasman JW, Beckmann CF, van de Warrenburg BP. Task-free functional MRI in cervical dystonia reveals multi-network changes that partially normalize with botulinum toxin. *PloS One* 2013;8(5):e62877.
- de Vries PM, Johnson KA, de Jong BM, et al. Changed patterns of cerebral activation related to clinically normal hand movement in cervical dystonia. *Clin Neurol Neurosurg* 2008;110(2):120–128.
- Prudente CN, Hess EJ, Jinnah H. Dystonia as a network disorder: what is the role of the cerebellum? *Neuroscience* 2014;260:23–35.
- Ramdhani RA, Simonyan K. Primary dystonia: conceptualizing the disorder through a structural brain imaging lens. *Tremor Other Hyperkinet Mov* 2013;3:tre-03-152-3638-4.
- Colosimo C, Pantano P, Calistri V, Totaro P, Fabbrini G, Berardelli A. Diffusion tensor imaging in primary cervical dystonia. *J Neurol Neurosurg Psychiatry* 2005;76(11):1591–1593.
- Bonilha L, de Vries PM, Vincent DJ, et al. Structural white matter abnormalities in patients with idiopathic dystonia. *Mov Disord* 2007;22(8):1110–1116.
- Fabbrini G, Pantano P, Totaro P, et al. Diffusion tensor imaging in patients with primary cervical dystonia and in patients with blepharospasm. *Eur J Neurol* 2008;15(2):185–189.
- Raffelt DA, Smith RE, Ridgway GR, et al. Connectivity-based fixel enhancement: whole-brain statistical analysis of diffusion MRI measures in the presence of crossing fibres. *Neuroimage* 2015;117:40–55.
- Jeurissen B, Leemans A, Tournier JD, Jones DK, Sijbers J. Investigating the prevalence of complex fiber configurations in white matter tissue with diffusion magnetic resonance imaging. *Hum Brain Mapp* 2013;34(11):2747–2766.
- Raffelt DA, Tournier J-D, Smith RE, et al. Investigating white matter fibre density and morphology using fixel-based analysis. *Neuroimage* 2017;144:58–73.
- Mito R, Raffelt D, Dholander T, et al. Fibre-specific white matter reductions in Alzheimer's disease and mild cognitive impairment. *Brain* 2018;141(3):888–902.

21. Gajamange S, Raffelt D, Dhollander T, et al. Fibre-specific white matter changes in multiple sclerosis patients with optic neuritis. *NeuroImage Clin* 2018;17:60–68.
22. Albanese A, Bhatia K, Bressman SB, et al. Phenomenology and classification of dystonia: a consensus update. *Mov Disord* 2013;28(7):863–873.
23. Consky E, Basinski A, Belle L, Ranawaya R, Lang A. The Toronto Western Spasmodic Torticollis Rating Scale (TWSTRS): assessment of validity and inter-rater reliability. *Neurology* 1990;40(suppl 1):445.
24. Beck AT, Steer RA, Brown GK. Beck Depression Inventory. Washington, DC: American Psychological Association; 1996.
25. Kaufman AS, Lichtenberger EO. Assessing Adolescent and Adult Intelligence. Hoboken, NJ: John Wiley & Sons; 2005.
26. O'Brien KR, Kober T, Hagmann P, et al. Robust T1-weighted structural brain imaging and morphometry at 7T using MP2RAGE. *PloS One* 2014;9(6):e99676.
27. Marques J. Retrieved from <https://github.com/JosePMarques/MP2RAGE-related-scripts>
28. Andersson JL, Sotiropoulos SN. An integrated approach to correction for off-resonance effects and subject movement in diffusion MR imaging. *Neuroimage* 2016;125:1063–1078.
29. Tournier J-D, Smith R, Raffelt D, et al. MRtrix3: a fast, flexible and open software framework for medical image processing and visualisation. *Neuroimage* 2019;202:116137.
30. Andersson JL, Skare S, Ashburner J. How to correct susceptibility distortions in spin-echo echo-planar images: application to diffusion tensor imaging. *Neuroimage* 2003;20(2):870–888.
31. Zhang H, Schneider T, Wheeler-Kingshott CA, Alexander DC. NODDI: practical in vivo neurite orientation dispersion and density imaging of the human brain. *Neuroimage* 2012;61(4):1000–1016.
32. Smith RE, Tournier J-D, Calamante F, Connelly A. SIFT: Spherical-deconvolution informed filtering of tractograms. *Neuroimage* 2013;67:298–312.
33. Fan L, Li H, Zhuo J, et al. The human brainnetome atlas: a new brain atlas based on connectional architecture. *Cereb Cortex* 2016;26(8):3508–3526.
34. Diedrichsen J. A spatially unbiased atlas template of the human cerebellum. *Neuroimage* 2006;33(1):127–138.
35. Winkler AM, Ridgway GR, Webster MA, Smith SM, Nichols TE. Permutation inference for the general linear model. *Neuroimage* 2014;92:381–397.
36. Behrens TE, Berg HJ, Jbabdi S, Rushworth MF, Woolrich MW. Probabilistic diffusion tractography with multiple fibre orientations: What can we gain? *Neuroimage* 2007;34(1):144–155.
37. Tsai S-Y. Reproducibility of structural brain connectivity and network metrics using probabilistic diffusion tractography. *Sci Rep* 2018;8(1):1–12.
38. Gong G, Rosa-Neto P, Carbonell F, Chen ZJ, He Y, Evans AC. Age- and gender-related differences in the cortical anatomical network. *J Neurosci* 2009;29(50):15684–15693.
39. Cao Q, Shu N, An L, et al. Probabilistic diffusion tractography and graph theory analysis reveal abnormal white matter structural connectivity networks in drug-naïve boys with attention deficit/hyperactivity disorder. *J Neurosci* 2013;33(26):10676–10687.
40. Rubinov M, Sporns O. Complex network measures of brain connectivity: uses and interpretations. *Neuroimage* 2010;52(3):1059–1069.
41. Hanekamp S, Simonyan K. The large-scale structural connectome of task-specific focal dystonia. *Hum Brain Mapp* 2020;41(12):3253–3265.
42. Johansen-Berg H, Behrens TE. Diffusion MRI: From Quantitative Measurement to In Vivo Neuroanatomy. Oxford, UK: Academic Press; 2013.
43. Zatorre RJ, Fields RD, Johansen-Berg H. Plasticity in gray and white: neuroimaging changes in brain structure during learning. *Nat Neurosci* 2012;15(4):528–536.
44. Dhollander T, Clemente A, Singh M, et al. Fixel-based analysis of diffusion MRI: methods, applications, challenges and opportunities. *Neuroimage* 2021;241:118417.
45. Pannek K, Frupp J, George JM, et al. Fixel-based analysis reveals alterations in brain microstructure and macrostructure of preterm-born infants at term equivalent age. *NeuroImage Clin* 2018;18:51–59.
46. Carandini T, Mancini M, Bogdan I, et al. Disruption of brainstem monoaminergic fibre tracts in multiple sclerosis as a putative mechanism for cognitive fatigue: a fixel-based analysis. *NeuroImage Clin* 2021;30:102587.
47. Zito GA, Tarrano C, Jegatheesan P, et al. Somatotopy of cervical dystonia in motor-cerebellar networks: evidence from resting state fMRI. *Parkinsonism Relat Disord* 2022;94:30–36.
48. Huang X, Zhang M, Li B, Shang H, Yang J. Structural and functional brain abnormalities in idiopathic cervical dystonia: a multimodal meta-analysis. *Parkinsonism Relat Disord* 2022;103:153–165.
49. Delnooz C, Pasman JW, Beckmann CF, van de Warrenburg BP. Altered striatal and pallidal connectivity in cervical dystonia. *Brain Struct Funct* 2015;220(1):513–523.
50. Conte A, Defazio G, Hallett M, Fabbri G, Berardelli A. The role of sensory information in the pathophysiology of focal dystonias. *Nat Rev Neurol* 2019;15(4):224–233.
51. Feng L, Yin D, Wang X, et al. Brain connectivity abnormalities and treatment-induced restorations in patients with cervical dystonia. *Eur J Neurol* 2021;28(5):1537–1547.
52. Berman BD, Pollard RT, Shelton E, Karki R, Smith-Jones PM, Miao Y. GABAA receptor availability changes underlie symptoms in isolated cervical dystonia. *Front Neurol* 2018;9:188.
53. Pan P, Wei S, Ou Y, et al. Reduced global-brain functional connectivity and its relationship with symptomatic severity in cervical dystonia. *Front Neurol* 2020;10:1358.
54. Berlucchi G, Aglioti S. The body in the brain: neural bases of corporeal awareness. *Trends Neurosci* 1997;20(12):560–564.
55. Berti A, Bottini G, Gandola M, et al. Shared cortical anatomy for motor awareness and motor control. *Science* 2005;309(5733):488–491.
56. Moro V, Pernigo S, Tsakiris M, et al. Motor versus body awareness: voxel-based lesion analysis in anosognosia for hemiplegia and somatoparaphrenia following right hemisphere stroke. *Cortex* 2016;83:62–77.
57. Naito E, Morita T, Amemiya K. Body representations in the human brain revealed by kinesthetic illusions and their essential contributions to motor control and corporeal awareness. *Neurosci Res* 2016;104:16–30.
58. Naito E, Morita T, Saito DN, et al. Development of right-hemispheric dominance of inferior parietal lobule in proprioceptive illusion task. *Cereb Cortex* 2017;27(11):5385–5397.
59. Desmurget M, Reilly KT, Richard N, Szathmari A, Mottolese C, Sirigu A. Movement intention after parietal cortex stimulation in humans. *Science* 2009;324(5928):811–813.
60. Burks JD, Boettcher LB, Conner AK, et al. White matter connections of the inferior parietal lobule: a study of surgical anatomy. *Brain Behav* 2017;7(4):e00640.
61. Porcacchia P, Palomar FJ, Cáceres-Redondo MT, et al. Parieto-motor cortical dysfunction in primary cervical dystonia. *Brain Stimul* 2014;7(5):650–657.
62. Bianchi S, Fuertinger S, Huddleston H, Frucht SJ, Simonyan K. Functional and structural neural bases of task specificity in isolated focal dystonia. *Mov Disord* 2019;34(4):555–563.
63. Van Der Werf J, Jensen O, Fries P, Medendorp WP. Neuronal synchronization in human posterior parietal cortex during reach planning. *J Neurosci* 2010;30(4):1402–1412.
64. Vicario C, Martino D, Koch G. Temporal accuracy and variability in the left and right posterior parietal cortex. *Neuroscience* 2013;245:121–128.
65. Rizzolatti G, Fogassi L, Gallese V. Neurophysiological mechanisms underlying the understanding and imitation of action. *Nat Rev Neurosci* 2001;2(9):661–670.

66. Jeannerod M, Arbib MA, Rizzolatti G, Sakata H. Grasping objects: the cortical mechanisms of visuomotor transformation. *Trends Neurosci* 1995;18(7):314–320.
67. Merchant SHI, Frangos E, Parker J, et al. The role of the inferior parietal lobule in writer's cramp. *Brain* 2020;143(6):1766–1779.
68. Gallea C, Horovitz SG, Ali Najee-Ullah M, Hallett M. Impairment of a parieto-premotor network specialized for handwriting in writer's cramp. *Hum Brain Mapp* 2016;37(12):4363–4375.
69. Jinnah H, Hess EJ. A new twist on the anatomy of dystonia: the basal ganglia and the cerebellum? *Neurology* 2006;67(10):1740–1741.
70. Filip P, Gallea C, Lehericy S, et al. Disruption in cerebellar and basal ganglia networks during a visuospatial task in cervical dystonia. *Mov Disord* 2017;32(5):757–768.

Supporting Data

Additional Supporting Information may be found in the online version of this article at the publisher's web-site.